Dizerens, C., S. Lenggenhager, M. Schwander, A. Buck, and S. Foffa (2017) The 1956 Cold Wave in Western Europe. In: Brönnimann, S. (Ed.) *Historical Weather Extremes in Reanalyses.* Geographica Bernensia G92, p. 101-111, DOI: 10.4480/GB2017.G92.09

The 1956 Cold Wave in Western Europe

Céline Dizerens*, Sina Lenggenhager, Mikhaël Schwander, Annika Buck and Selina Foffa

Oeschger Centre for Climate Change Research and Institute of Geography, University of Bern, Switzerland

Abstract

In February 1956, a severe cold wave occurred in Western Europe that led to exceptionally low temperatures and to one of the lowest monthly temperature averages in Western and Southern Europe on record. In this study, we analyze the meteorological situation that was leading to this cold wave using the Twentieth Century Reanalysis (20CRv2c) and an experimental reanalysis, called ERA-PreSAT. Pressure, temperature and geopotential height from 20CRv2c and ERA-PreSAT are used to examine the synoptic situation during the cold wave. Additionally, the performance of the reanalysis data is assessed by comparing it to temperature measurements from station data and historical weather charts from the *Monthly Weather Review*. We find that the cold wave was connected to a long-lasting blocking event over Europe, which continuously advected cold polar air to Western Europe. We conclude that the reanalysis is able to reproduce the large-scale characteristics of the cold wave in February 1956.

1. Introduction

In February 1956, a severe cold wave occurred in Western Europe. Andrews (1956) described this cold wave as the worst of the century, and according to Pfister (1999), February 1956 is remembered as one of the coldest months on record. Eastern France, Southern Germany, Switzerland, and Austria were particularly strongly affected. The low temperatures let lakes and rivers freeze and caused plant damages and fatalities. Between 13 and 29 February, shipping on the Rhine river was stopped as the Rhone-Rhine Canal and the Rhine river in the lower and middle Rhine region were frozen (see Fig. 1). Ports in the Basel region were

* Corresponding author: Céline Dizerens, University of Bern, Institute of Geography, Hallerstr. 12, CH-3012 Bern, Switzerland. E-mail: celine.dizerens@giub.unibe.ch

blocked by a thick ice cover (Canton of Basel-Landschaft, 1956). Mean temperature anomalies were clearly below normal over all of Europe, with greatest anomalies measured in Zurich (monthly mean -4.4°C below normal) and extremely low temperatures measured near the Swiss-Italian border (minima down to -42.7 °C) and in northern Sweden (-40°C) (Andrews, 1956).

The aim of this study is to analyze this cold wave using version 2c of the "Twentieth Century Reanalysis" (20CRv2c, Compo et al., 2011) and an experimental reanalysis, called ERA-PreSAT (Hersbach et al., 2017). According to Andrews (1956), the event is closely related to a pronounced and persistent blocking in the North Atlantic and Eurasia, which led to an extreme abnormality in the hemispheric circulation pattern.

To our knowledge, the 1956 cold wave event has not been studied extensively. Hirschi and Sinha (2007) analyzed winter temperature anomalies for six cold winters between 1948 and 2006 including the winter in 1956 using the NCEP/NCAR reanalysis dataset. However, they mainly analyzed the whole winter season 1956 and focus on its monthly temperature anomalies in western Russia only.

In this study, we use pressure, temperature and geopotential height from 20CRv2c and ERA-PreSAT to analyze the synoptic evolution that led to the cold wave. Additionally, we compare our reanalysis data with historical weather charts and temperature measurements from station data to investigate how well 20CRv2c and ERA-PreSAT are able to reconstruct the cold wave event in February 1956.

The paper is organized as follows. In Section 2, 20CRv2c, ERA-PreSAT, and the historical observations are introduced. In Section 3, we present the meteorological situation as depicted in 20CRv2c and ERA-PreSAT, followed by a comparison of the reanalysis data to historical weather charts and station measurements. In Section 5, we discuss the results. Conclusions are drawn in Section 6.

Figure 1. Frozen Rhine river in Mainz with a view on the Theodor-Heuss bridge in February 1956 (Photo courtesy: Federal Waterways Engineering and Research Institute BAW).

2. Data and Methods

The Twentieth Century Reanalysis version 2c (20CRv2c) and ERA-PreSAT reanalysis data are used in this study. 20CRv2c is the latest version of 20CR, which is a global three-dimensional atmospheric dataset covering the period from 1871 to 2010 (Compo et al., 2011). 20CRv2c was released in 2015 and reaches back to 1851. It is based on surface and sea-level pressure from the International Surface Pressure Database (ISPD) version 3.2.9 (Cram et al., 2015), which were assimilated into the NCEP/CFS forecasting model using a variant of the Ensemble Kalman Filter (Saha et al., 2010), forced by sea-surface temperature and sea ice from the Simple Ocean Data Assimilation with sparse input (SODAsi, Giese et al., 2016) and COBE sea-surface temperatures (Hirahara et al., 2014). 20CRv2c has a 6-hourly temporal resolution, a spatial resolution of 2° by 2°, and consists of 56 ensemble members. For more detailed information on this and other reanalyses used in this book see Brönnimann (2017). In this study, we will investigate the ensemble mean only as the ensemble spread of temperature and geopotential height is small due to the dense network of observation data that was assimilated in the time-period of the cold wave (see Fig. 2).

While 20CRv2 only assimilates observations of surface and sea-level pressure, ERA-PreSAT additionally uses marine winds and upper-air observations from the CHUAN historical dataset (Stickler et al., 2010) that are supplemented by data from the upper-air archives at the National Center for Atmospheric Research (NCAR) (Hersbach et al., 2017). ERA-PreSAT covers the years 1939-1967. It has a spatial resolution of 1° by 1° and a six-hourly temporal resolution.

To investigate the synoptic development, we use geopotential height at 500 hPa and temperature at 850 hPa from the two reanalyses 20CRv2c and ERA-PreSAT. Geopotential height anomalies at 200 hPa are used to identify atmospheric blockings during the cold wave event. For 20CRv2c data, the blocking index RO200 proposed by Rohrer (2017) is used.

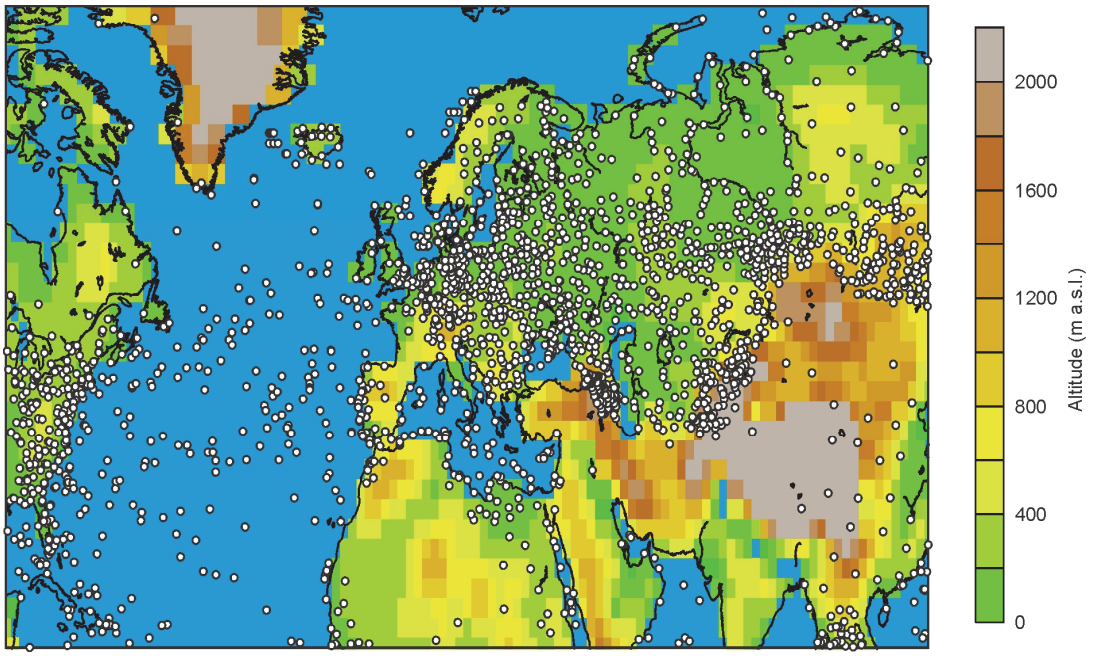

Figure 2. Topography of the 20CRv2c dataset. White dots show all observations assimilated into 20CRv2c for 1 February 1956, 12 UTC.

We use a slightly different definition of a block than Andrews (1956), who defines blocking as a closed high-pressure isobar in the 5-day running mean of the 700 hPa geopotential height that is located north of 45°N. In our study, we define blockings as persistent positive anomalies of geopotential height at 200 hPa, following the methodology of Rohrer (2017). To be considered a block, the anomalies need to persist for at least 5 days with a spatial overlap of at least 70% of the area between two time steps.

Temperature at 850 hPa is compared to a historical weather chart from Andrews (1956). Moreover, 2-m air temperature from 20CRv2c and ERA-PreSAT are compared with daily temperature measurements from the stations in Basel (Switzerland) and Marseille (France), obtained from the European Climate Assessment & Dataset project (ECA&D, Klein Tank et al. 2002).

3. Results

3.1. Synoptic overview

In the following, we analyze the blocking situation in February 1956 using geopotential height from 20CRv2c and ERA-PreSAT. The blocking density in February 1956 is derived from 20CRv2c (Fig. 3). It shows two maxima, one is high in the North Atlantic and one over Northern Russia. The values of up to 70% show that in more than two thirds of the time a block was present over Northern Russia. This very high blocking density indicates a highly persistent blocking situation during most of the month.

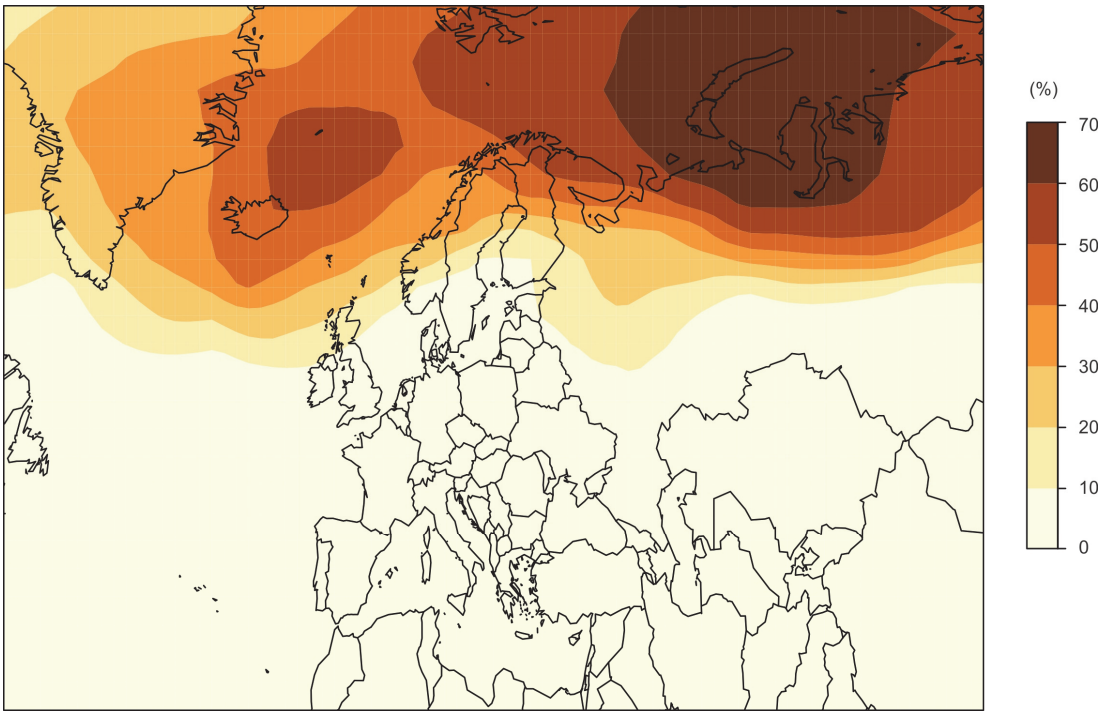

Figure 3. Blocking density [%] in February 1956, as detected by the RO200 blocking index in the 20CRv2c dataset.

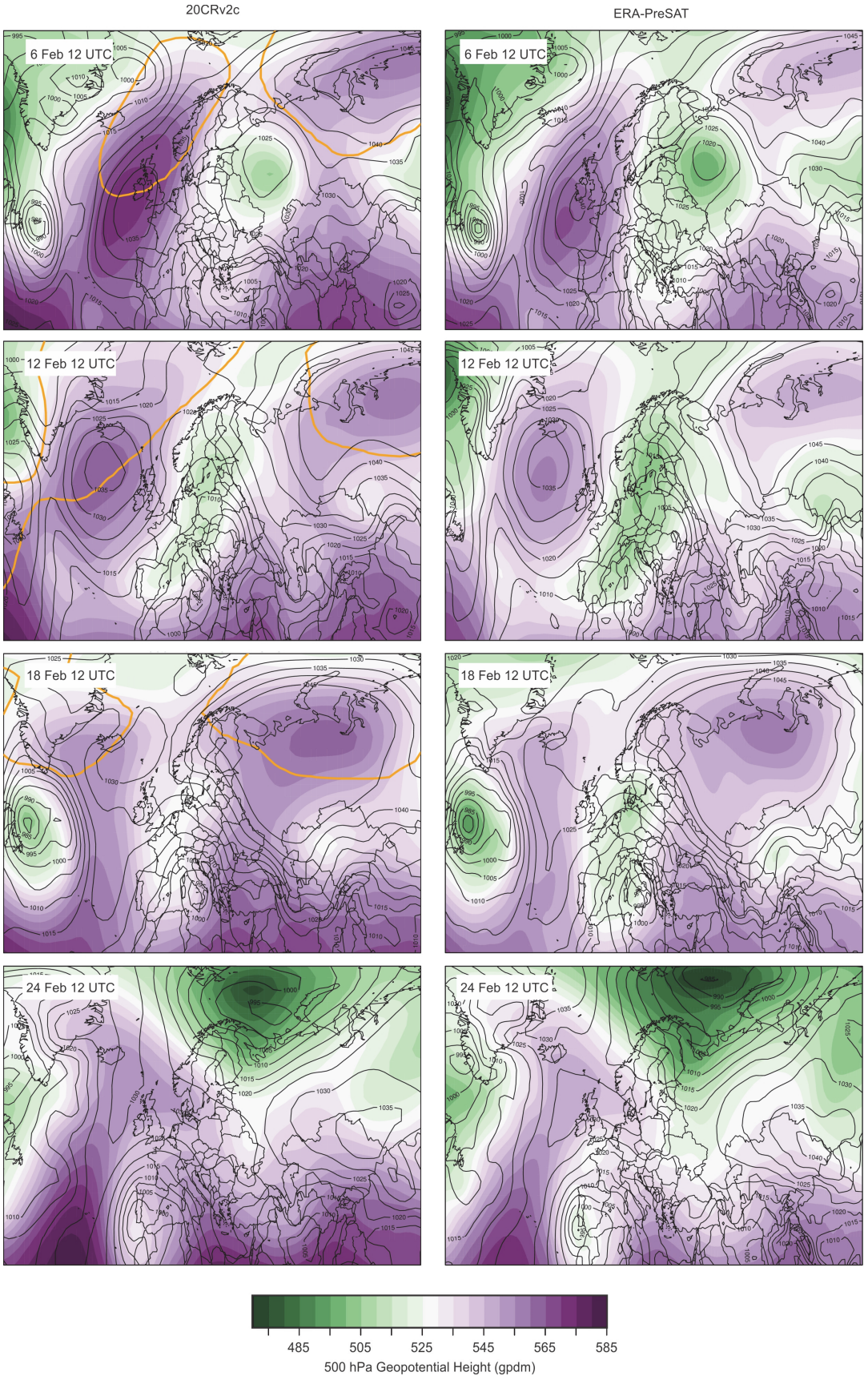

Figure 4. Geopotential height at 500 hPa (shaded colors) and sea-level pressure in hPa (contours) from 20CRv2c (left) and ERA-PreSAT (right) for 6, 12, 18, and 24 February 1956. The location of the detected blockings is shown for 20CR as orange contours. For 20CRv2c, the ensemble mean is shown.

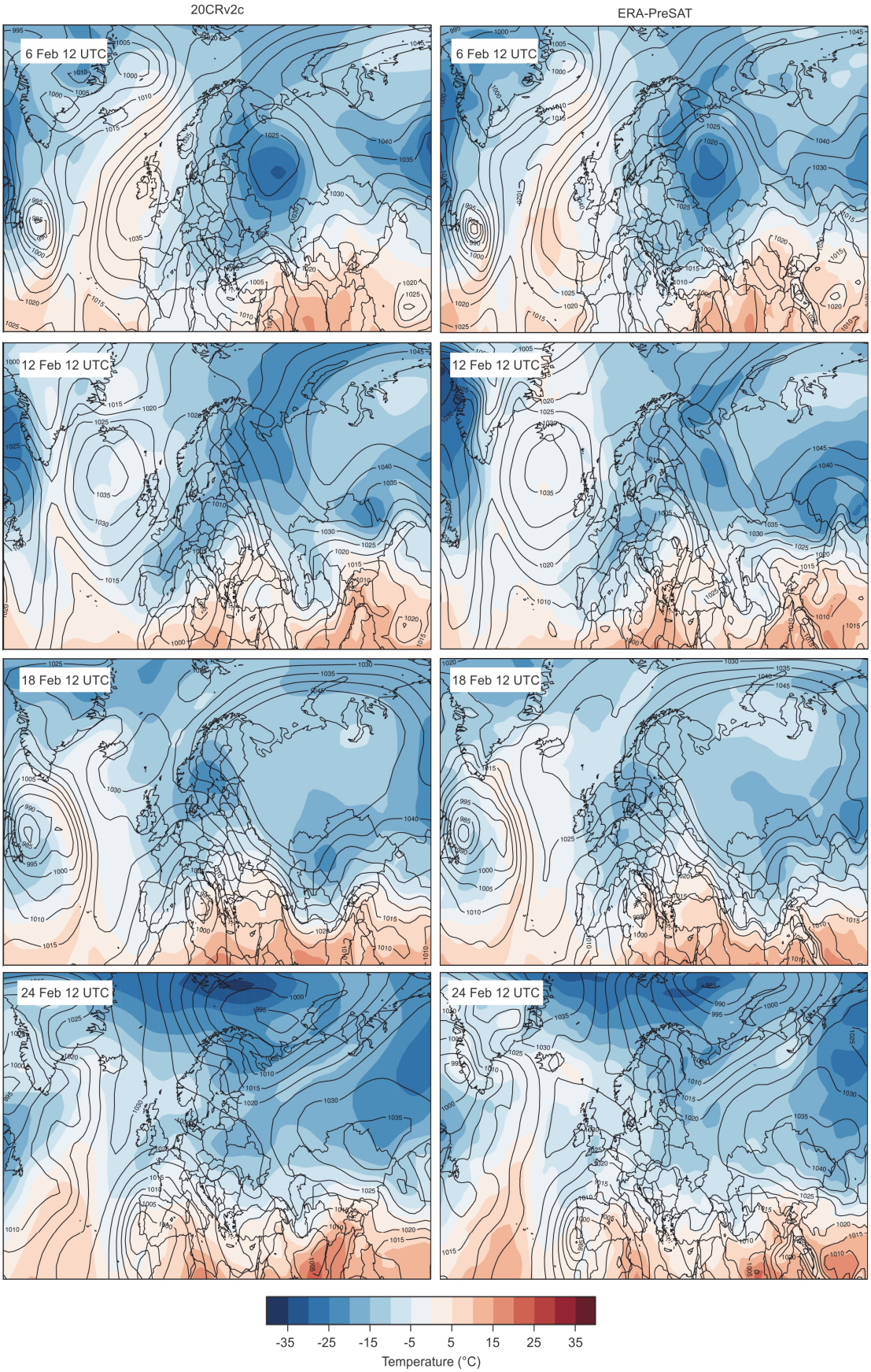

Figure 5. Temperature at 850 hPa in degrees Celsius (shaded colors) and sea-level pressure in hPa (contours) from 20CRv2c (left) and ERA-PreSAT (right) for 6, 12, 18, and 24 February 1956. For 20CRv2c, the ensemble mean is shown.

We analyze the synoptic situation for 6, 12, 18, and 24 February 1956 at 12 UTC using geopotential height at 500 hPa and sea-level pressure for 20CRv2c and ERA-PreSAT (Fig. 4). The location of the blockings is depicted in orange contours and is calculated for 20CRv2c only. Between 1 and 23 February, two strong mid-tropospheric ridges can be observed over the North Atlantic and Russia. In between the two systems, a cut-off low was located over eastern Europe. Both of the two mid-tropospheric high pressure systems were associated with an upper-level blocking. This double-block was more or less persistent from 1 to 23 February 1956. The cut off-low was reattached a few days later and formed a meridionally elongated weak trough over central Europe. This trough was locked in between the two blocking systems and therefore also remained stationary. At the eastern flank of the ridges, the constant advection of cold polar air towards the south caused this very long-lasting and intense cold wave.

Temperature at 850 hPa for 20CRv2c and ERA-PreSAT is shown in Figure 5. Both reanalysis datasets are able to roughly approximate reported temperature minima. The strong high pressure system over the North Atlantic led to cold air masses that are moved over Western Europe, while warm air was advected northwards west of the North Atlantic blocking. After 24 February, temperatures slowly increased in Western Europe.

3.2. Comparison of historical temperature data with 20CRv2c and ERA-PreSAT reanalyses

We compare the monthly mean surface temperature anomaly from the *Monthly Weather Review* (Andrews, 1956) with the ensemble mean of monthly mean 2-metre air temperature anomaly calculated for 20CRv2c (Fig. 6). The reconstructions from 20CRv2c show a similar pattern of temperature anomaly than the temperature anomaly of the *Monthly Weather Review*. However, the centre of the low temperature anomaly is located over central France in 20CRv2c, whereas the centre of low temperature anomaly from the *Monthly Weather Review* lies over Switzerland and Southern Germany.

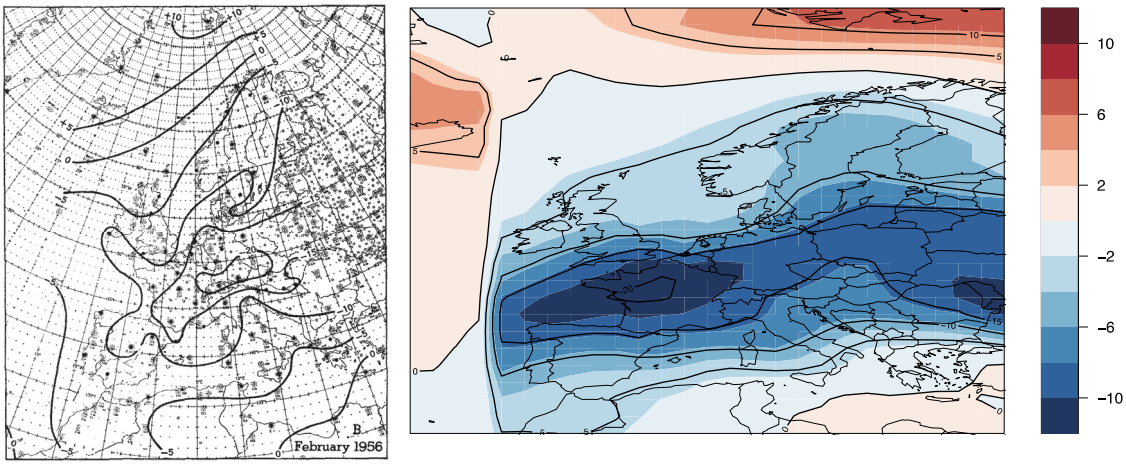

Figure 6. (left) Monthly mean surface temperature anomaly from the *Monthly Weather Review* (Andrews, 1956) in degrees Fahrenheit (contours) and (right) ensemble mean of monthly mean 2-metre air temperature anomaly from 20CRv2c in degrees Fahrenheit (contours) and degrees Celsius (shading). The 20CRv2c anomaly is calculated relative to the 1931 to 1960 climatology, whereas the temperature anomaly from the *Monthly Weather Review* is based on a 30-year average (1901-1930) of available station data (solid dots).

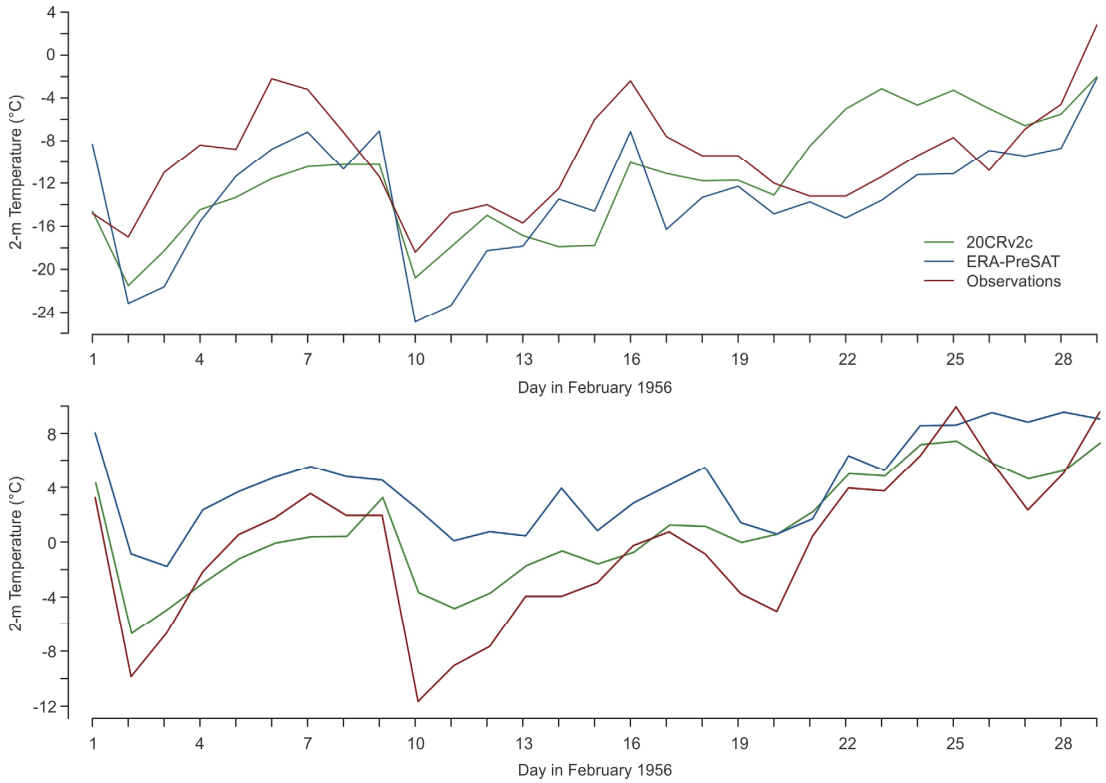

Figure 7. Time series of 2-m temperature at the locations of (top) Basel and (bottom) Marseille for 20CRv2c (green) and ERA-PreSAT (blue) in comparison with observations in the ECA&D data set (red).

In the following, we examine the time series of the two grid boxes that include the measurement station in Basel (CH) and Marseille (FR) in the 20CRv2c and ERA-PreSAT reanalyses. The time series of 2-metre daily mean temperature in February for 20CRv2c and ERA-PreSAT are compared to temperature data from the measurement station in Basel (Fig. 7, top). Both reanalyses are able to reproduce the main temperature development in Basel including the three major temperature drops. During the temperature minima, mean temperatures in 20CR and ERA-PreSAT are, however, between 2 °C and 7 °C lower than in the observations. Except for these minima, ERA-PreSAT temperature better matches the observational data than 20CRv2c, especially between 20 and 27 February, where the 20CRv2c temperature suddenly increases on 20 February and remained 5 to 6 days between 4°C and 8°C higher compared to the station measurements.

The reverse result is observed when comparing the 2-metre temperature of the reanalysis data to temperature observations from Marseille (Fig. 7, bottom). Temperatures from 20CRv2c and ERA-PreSAT are between 1°C and 12°C warmer than the station data. Especially during the main temperature drops, the reanalysis data deviate from the temperature measurements in Marseille. Despite the coarser spatial resolution of 20CRv2c compared to ERA-PreSAT, 20CRv2c better approximates the observed station temperature data.

4. Discussion

The long-lasting blocking situation is well depicted in 20CRv2c and is similar to the blocking patterns observed by Andrews (1956). Andrews (1956) observed a maximum block intensity between 15 and 19 February 1956. In addition, he reported that the duration of the blocking situation is considerably longer than the average duration of 16 days for a winter block. The same can be observed in 20CRv2c, where the duration of the blocking situation is 23 days using the blocking index RO200. However, the block intensity in 20CRv2c is rather weak between 15 and 17 February.

Generally, we find a good agreement between the 20CRv2c and ERA-PreSAT reanalysis datasets. Both reanalyses show similar patterns in pressure distribution (see Fig. 4). However, the low pressure system over Europe is stronger in ERA-PreSAT compared to 20CRv2c: whereas the low pressure system in 20CRv2c attained values of about 515 gdm, the low pressure system in ERA-PreSAT reaches values of about 500 gdm. In addition, the two mid-tropospheric ridges are more pronounced in 20CRv2c compared to ERA-PreSAT, especially during the first half of February. Small differences can be also observed in the temperature reconstructions, where the advection of cold polar air towards the south generally results in lower temperature values in 20CRv2c compared to ERA-PreSAT.

The temperature and pressure data from 20CRv2c and ERA-PreSAT show a good agreement with the historical weather chart and the station measurements in Basel and Marseille. The monthly mean 2-metre air temperature anomaly from 20CRv2c agrees well with the mean temperature anomaly of the *Monthly Weather Review* map. Despite the more western location of the minimum temperature anomaly, the 20CRv2c anomaly shows the same large-scale pattern as the *Monthly Weather Review* temperature anomaly.

Two-metre daily mean temperature from 20CRv2c and ERA-PreSAT provides a good approximation of the daily temperature measurements from the measurement station in Basel and Marseille. Despite the coarse resolution of the reanalyses, temperature drops are well depicted in 20CRv2c and ERA-PreSAT. This can be attributed to the dense observation network assimilated in the reanalyses. However, the comparisons for the two stations reveals differences: whereas reanalysis temperature in Basel are generally too low compared to observations – especially for strong temperature drops – reanalysis temperature in Marseille are higher than the temperature observations and the temperature drops are less well pronounced in the reanalysis data. A reason for this could be that most of the selected grid point for Marseille lies over the sea and therefore, fast temperature changes are not well depicted in the reanalysis data of this grid cell.

The comparison between 20CRv2c and ERA-PreSAT shows only slight differences, with no clear winner. The surface information in 1956 seems to be dense enough to allow a good representation of the general atmospheric conditions. Conversely, upper-air information does not improve the situation with respect to local minimum temperatures.

5. Conclusions

We have shown that 20CRv2v and ERA-PreSAT are able to reproduce the large-scale characteristics of the cold wave in February 1956 and that the development of the blocking phenomena is well depicted in both reanalyses. Observed blocking patterns are comparable to

the findings shown by Andrews (1956) and show a long-lasting blocking event over Europe, which continuously advected cold polar air to Western Europe. We have found a good agreement between the 20CRv2c and ERA-PreSAT reanalysis datasets. Despite the coarse resolution of the reanalyses, regional temperature changes are well depicted and agree well with historical weather charts and station measurements.

Acknowledgements

The Twentieth Century Reanalysis Project dataset was obtained courtesy of the NOAA/OAR/ESRL PSD, Boulder, Colorado, USA, from their web page at http://www.esrl.noaa.gov/psd/. Support for the 20CR dataset is provided by the U.S. Department of Energy, Office of Science Innovative and Novel Computational Impact on Theory and Experiment program, Office of Biological and Environmental Research and by the National Oceanic and Atmospheric Administration Climate Program Office. The work was supported by FP7 project ERA-CLIM2, H2020 project EUSTACE, and the Swiss National Science Foundation projects 200021_156059 and 200021_143219.

References

Andrews, J. F. (1956) The Weather and Circulation of February 1956. *Monthly Weather Rreview,* **84,** 66–74.

Brönnimann, S. (2017) Weather Extremes in an Ensemble of Historical Reanalyses. In: Brönnimann, S. (Ed.) *Historical Weather Extremes in Reanalyses.* Geographica Bernensia G92, p. 7-22, DOI: 10.4480/GB2017.G92.01.

Canton of Basel-Landschaft (1956) Chronicle of the Canton of Basel-Landschaft. Retrieved from https://www.baselland.ch/themen/c_d/chronik-bl/chronik-1950er/chronik-1956/chronik-februar-1956

Compo, G. P., J. S. Whitaker, P. D. Sardeshmukh, N. Matsui, R. J. Allan, X. Yin, B. E. Gleason, R. S. Vose, G. Rutledge, P. Bessemoulin, S. Brönnimann, M. Brunet, R. I. Crouthamel, A. N. Grant, P. Y. Groisman, P. D. Jones, M. Kruk, A. C. Kruger, G. J. Marshall, M. Maugeri, H. Y. Mok, Ø. Nordli, T. F. Ross, R. M. Trigo, X. Wang, S. D. Woodruff, and S. J. Worley (2011) The Twentieth Century Reanalysis Project. *Q. J. R. Meteorol. Soc.,* **137,** 1-28.

Cram, T. A., G. P. Compo, X. G. Yin, R. J. Allan, C. McColl, R. S. Vose, J. S. Whitaker, N. Matsui, L. Ashcroft, R. Auchmann, P. Bessemoulin, T. Brandsma, P. Brohan, M. Brunet, J. Comeaux, R. Crouthamel, B. E. Gleason, P. Y. Groisman, H. Hersbach, P. D. Jones, T. Jonsson, S. Jourdain, G. Kelly, K. R. Knapp, A. Kruger, H. Kubota G. Lentini, A. Lorrey, N. Lott, S. J. Lubker, J. Luterbacher, G. J. Marshall, M. Maugeri, C. J. Mock, H. Y. Mok, O. Nordli, M. J. Rodwell, T. F. Ross, D. Schuster, L. Srnec, M. A. Valente, Z. Vizi, X. L. Wang, N. Westcott, J. S. Woollen, and S. J. Worley (2015) The International Surface Pressure Databank version 2. *Geosci. Data J.,* **2,** 31–46, doi:10.1002/gdj3.25.

Giese, B. S., H. F. Seidel, G. P. Compo, and P. D. Sardeshmukh (2016) An ensemble of ocean reanalyses for 1815-2013 with sparse observational input. *J. Geophys. Res. Ocean.,* **121,** 6891–6910.

Hersbach H., S. Brönnimann, L. Haimberger, M. Mayer, L. Villiger, J. Comeaux, A. Simmons, D. Dee, S. Jourdain, C. Peubey, P. Poli, N. Rayner, A. M. Sterin, A. Stickler, M. A. Valente, and S. J. Worley (2017) The potential value of early (1939–1967) upper-air data in atmospheric climate reanalysis. *Q. J. R. Meteorol. Soc.,* **143,** 1197–1210.

Hirahara S., I. Masayoshi, and Y. Fukuda (2014) Centennial-scale sea surface temperature analysis and its uncertainty. *J. Climate,* **27,** 57–75.

Hirschi, J. J.-M and B. Sinha (2007) Negative NAO and cold Eurasian winters: how exceptional was the winter of 1962/1963? *Weather,* **62,** 43–48.

Klein Tank, A. M. G., J. B. Wijngaard, G. P. Können, R. Böhm, G. Demarée, A. Gocheva, M. Mileta, S. Pashiardis, L. Hejkrlik, C. Kern-Hansen, R. Heino, P. Bessemoulin, G. Müller-Westermeier, M. Tzanakou, S. Szalai, T. Pálsdóttir, D. Fitzgerald, S. Rubin, M. Capaldo, M. Maugeri, A. Leitass, A. Bukantis, R. Aberfeld, A. F. V. van Engelen, E. Forland, M. Mietus, F. Coelho, C. Mares, V. Razuvaev, E. Nieplova, T. Cegnar, J. Antonio López, B. Dahlström, A. Moberg, W. Kirchhofer, A. Ceylan, O. Pachaliuk, L. V. Alexander, and P. Petrovic (2002) Daily dataset of 20th-century surface air temperature and precipitation series for the European Climate Assessment. *Int. J. Climatol.,* **22,** 1441–1453.

Pfister, C. (1999) *Wetternachhersage. 500 Jahre Klimavariationen und Naturkatastrophen (1496-1995).* Verlag Paul Haupt, Bern, Stuttgart, Wien, 304 pp.

Rohrer, M. (2017) *Long-term changes in weather extremes in a large ensemble of climate model simulations.* PhD thesis, University of Bern.

Saha, S., S. Moorthi, H.-L. Pan, X. Wu, J. Wang, S. Nadiga, P. Tripp, R. Kistler, J. Woollen, D. Behringer, H. Liu, D. Stokes, R. Grumbine, G. Gayno, J. Wang, Y.-T. Hou, H.-Y. Chuang, H.-M. H. Juang, J. Sela, M. Iredell, R. Treadon, D. Kleist, P. Van Delst, D. Keyser, J. Derber, M. Ek, J. Meng, H. Wei, R. Yang, S. Lord, H. Van Den Dool, A. Kumar, W. Wang, C. Long, M. Chelliah, Y. Xue, B. Huang, J.-K. Schemm, W. Ebisuzaki, R. Lin, P. Xie, M. Chen, S. Zhou, W. Higgins, C.-Z. Zou, Qu. Liu, Y. Chen, Y. Han, L. Cucurull, R. W. Reynolds, G. Rutledge, and M. Goldberg (2010) The NCEP Climate Forecast System Reanalysis. *Bull. Amer. Meteorol. Soc.,* **91,** 1015–1057.

Stickler, A., A. Grant, T. Ewen, T. F. Ross, R. S. Vose, J. Comeaux, P. Bessemoulin, K. Jylhä, W. K. Adam, P. Jeannet, A. Nagurny, A. M. Sterin,R. Allan, G. P. Compo, T. Griesser, and S. Brönnimann (2010). The Comprehensive Historical Upper-Air Network. *Bull. Amer. Meteorol. Soc.,* **91,** 741–751.